Interface focus

J. R. Soc. Interface (2008) **5**, S151–S159
doi:10.1098/rsif.2008.0106.focus
Published online 2 June 2008

A cellular isolation system for real-time single-cell oxygen consumption monitoring

Joe Dragavon[1,*], Tim Molter[2], Cody Young[3,†], Tim Strovas[4,‡], Sarah McQuaide[2], Mark Holl[2,†], Meng Zhang[5], Brad Cookson[5,6], Alex Jen[7], Mary Lidstrom[6,8], Deirdre Meldrum[2,†] and Lloyd Burgess[1]

[1]*Department of Chemistry,* [2]*Department of Electrical Engineering,* [3]*Department of Physics,* [4]*Department of Bioengineering,* [5]*Department of Laboratory Medicine,* [6]*Department of Microbiology,* [7]*Department of Materials Science and Engineering, and* [8]*Department of Chemical Engineering, University of Washington, Seattle, WA 98195-2180, USA*

The development of a cellular isolation system (CIS) that enables the monitoring of single-cell oxygen consumption rates in real time is presented. The CIS was developed through a multidisciplinary effort within the Microscale Life Sciences Center (MLSC) at the University of Washington. The system comprises arrays of microwells containing Pt-porphyrin-embedded polystyrene microspheres as the reporter chemistry, a lid actuator system and a gated intensified imaging camera, all mounted on a temperature-stabilized confocal microscope platform. Oxygen consumption determination experiments were performed on RAW264.7 mouse macrophage cells as proof of principle. Repeatable and consistent measurements indicate that the oxygen measurements did not adversely affect the physiological state of the cells measured. The observation of physiological rates in real time allows studies of cell-to-cell heterogeneity in oxygen consumption rate to be performed. Such studies have implications in understanding the role of mitochondrial function in the progression of inflammatory-based diseases, and in diagnosing and treating such diseases.

Keywords: single-cell analysis; respiration rate; mouse macrophage

1. INTRODUCTION

Single-cell analysis has become an important tool in understanding fundamental cellular processes, due to the inherent heterogeneity of cellular populations (Kelly & Rahn 1932; Verstovsek *et al.* 1994; Kamme *et al.* 2003; Lidstrom & Meldrum 2003; Strovas *et al.* 2007). Averaged populations can obscure the existence of multiple physiological types that lead to variances in responses at the individual cell level (Balaban *et al.* 2004; Strovas *et al.* 2007). This in turn can result in incorrect data interpretation of major consequence, for instance involving the mechanism of action of a specific drug, the pathway whereby response occurs or the kinetics of response. The analysis of response at the single-cell level requires a system for making physiological measurements in living cells.

A parameter of significance for single-cell measurements is oxygen consumption rate. Oxygen consumption rate is a sensitive indicator of both steady-state physiological state and response to stimuli. In addition, changes in mitochondrial function are a hallmark of many inflammatory diseases such as cancer, stroke and heart disease (Fink & Cookson 2005). Therefore, the ability to measure oxygen consumption rate in single cells is an important technological step required for understanding the role of cellular heterogeneity in these diseases and in developing effective therapeutic interventions.

Multiple methods are known for monitoring oxygen concentrations in solution with the use of electrochemical methodologies being among the most common (Land *et al.* 1999; Lu & Gratzl 1999; Porterfield & Smith 2000; von Heimburg *et al.* 2005; Bugger *et al.* 2006; Gao *et al.* 2006). Clark oxygen electrodes are commonly used for cell culture monitoring (von Heimburg *et al.* 2005; Bugger *et al.* 2006) but are susceptible to drift due to fouling of the electrode and membrane interfaces, sensitivity to interfacial flow, consumption of oxygen during analysis and the difficulty in size reduction for single-cell measurements (Ramamoorthi & Lidstrom 1995; Reece *et al.* 2003; Strovas *et al.* 2006). Attempts to reduce the electrode size have met with some success (Lu & Gratzl 1999; Porterfield & Smith 2000; Yasukawa *et al.* 2000; Carano *et al.* 2003), but none have demonstrated a Clark-type electrode for diffusionally isolated single-cell analysis.

*Author and address for correspondence: Department of Chemistry, University of Hull, Hull HU6 7RX, UK (joedragavon@gmail.com).
†Present address: Center for Ecogenomics, The Biodesign Institute, Arizona State University, PO Box 875801, Tempe, AZ 85287-5801, USA.
‡Present address: Department of Electrical Engineering, University of Washington, Box 352500, Seattle, WA 98195, USA.

One contribution of 7 to a Theme Supplement 'Single-cell analysis'.

Received 14 March 2008
Accepted 15 May 2008

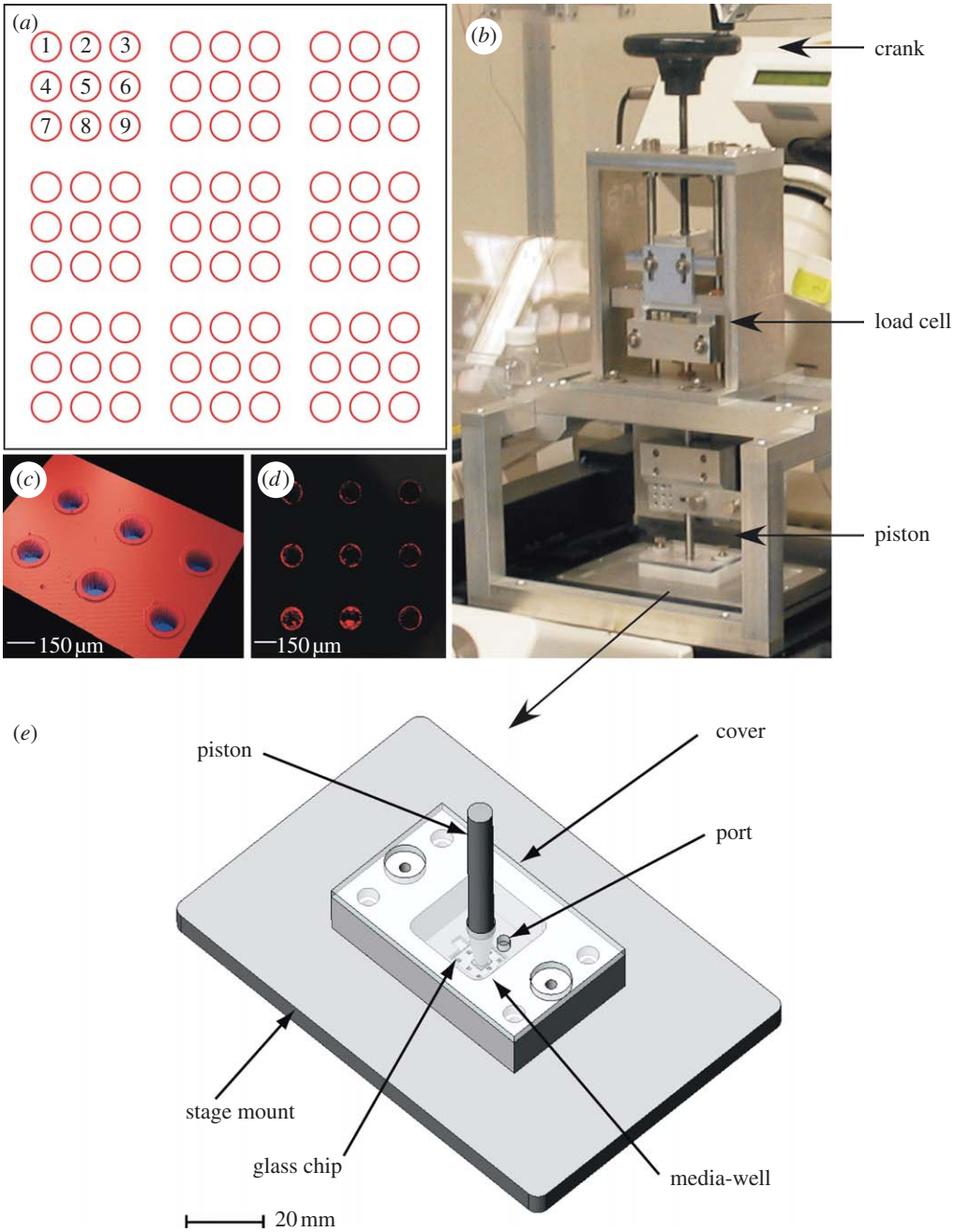

Figure 1. Images depicting (*a*) the layout of the microwell arrays etched into one borosilicate chip, (*b*) the actuator system, (*c*) an optical profilometer image showing the etched microwells with the lips clearly visible, (*d*) a laser scanning microscope (LSM) image of a microwell array showing the microsphere ring under excitation and (*e*) the living cell array (LCA). The LCA uses an aluminium plate to provide the support for a rigid quartz window. The quartz window was selected to provide adequate support to prevent the borosilicate chips from cracking under the load. (*b*) The actuator system acts as a manual linear actuator for the pistons. This system is advantageous since it removes instabilities and provides coaxial alignment of the piston to the borosilicate chip.

Recently, oxygen-sensitive porphyrin compounds have gained popularity as tools to monitor oxygen concentrations within fluids (Hartmann & Trettnak 1996; Lahdesmaki *et al.* 1999; Amao *et al.* 2000; Vinogradov *et al.* 2001; Armaroli 2003; Shonat & Kight 2003; Dy & Kasai 2005; Molter 2006; Molter *et al.* 2008). Pt-porphyrin-embedded polystyrene microspheres are commercially available and are attractive as oxygen sensors since they are biologically compatible (Strovas *et al.* 2006), have a good dynamic range and are easy to manipulate. As a proof of principle, a system was developed previously which demonstrated the feasibility of using these commercial microspheres as oxygen sensors for single-cell oxygen consumption rates (Molter *et al.* 2008).

In this study, we describe a robust cellular isolation system (CIS) that allows for the monitoring of oxygen consumption rates of many cells at once at the single-cell level. This system was demonstrated to allow reproducibility and repeatability in the measurement of single-cell oxygen consumption rates. These factors enable cell-to-cell heterogeneity to be directly addressed such that individual cells experience minimal perturbation during experimentation.

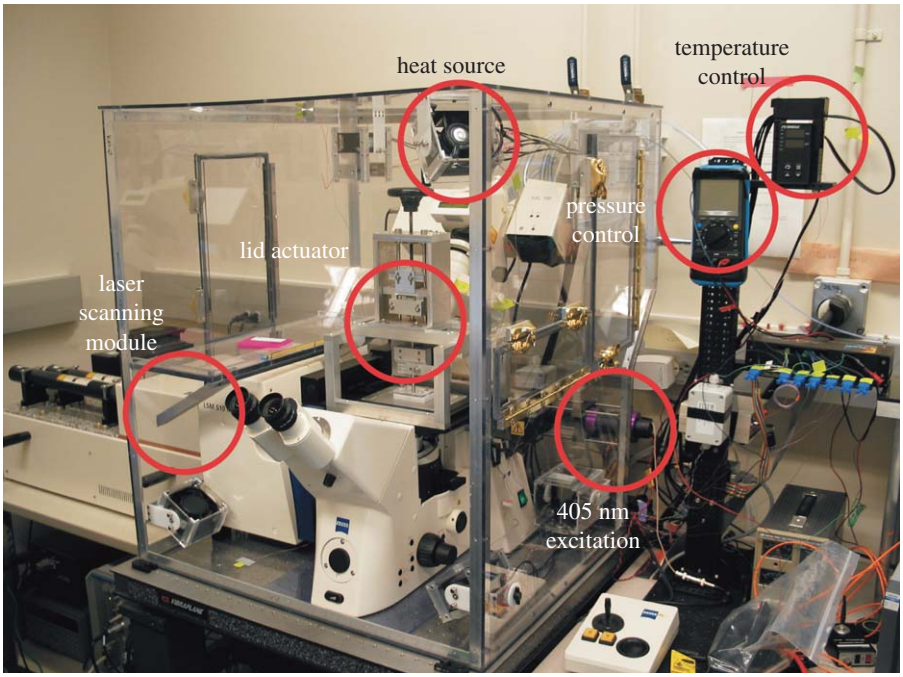

Figure 2. The current oxygen consumption monitoring system includes the LSM system, the actuator system (AS), the LCA and an environmental control system. The environmental control system includes three heater–fan modules to heat and circulate the air around the LCA through proportional–integral–derivative (PID) control and up to 12 thermocouples for temperature monitoring. The enclosure was designed to allow for easy access to all areas and provides shelf space for storing large media and reagent bottles. The red circles identify the item noted in the corresponding label.

2. MATERIAL AND METHODS

2.1. Microwell array

Standard photolithography techniques were used to etch 150 µm wide by 50 µm deep microwells into 1×1 cm borosilicate chips (figure 1). Steps were taken to produce microwells with a 30 µm wide by 3 µm high lip into a 3×3 array format (Molter *et al.* 2008). The lip surrounding each well provided a gasket-like ridge for optimal well sealing. Nine sets of 3×3 arrays were etched in 1×1 cm chips with the arrays spaced 2 mm apart from each other. Platinum luminescent fluorospheres (1 µm in diameter, $\lambda_{ex}=390$ nm, $\lambda_{em}=690$ nm, F-20888, Invitrogen, Carlsbad, CA, USA) were deposited into the microwells and used to monitor the oxygen concentration within each microwell (Molter *et al.* 2008). As described previously, this approach resulted in a sensor ring forming at the bottom of each well (Molter *et al.* 2008).

2.2. Living cell array

A large macrowell capable of holding approximately 8 ml of solution was made by combining a milled pocket in 1.25 cm thick polyacetal (Delrin, DuPont), which formed the side walls, and a 0.3 cm thick quartz window, which formed the base. The result is a 2.5×2.5×1.25 cm macrowell. A thin polydimethylsiloxane (PDMS) gasket was placed between the two components in order to form a leak-proof seal. The quartz window was supported by a 0.6 cm aluminium plate, with a central portion removed for optical access. Four screws were used to secure the macrowell to the aluminium plate. The aluminium plate had exterior dimensions that allow for easy mounting onto the microscope stage. A 0.3 cm piece of polycarbonate was used to cap the macrowell during experiments to reduce the evaporation of cell medium in the macrowell and retain a 20% O_2/5% CO_2/N_2 humidified atmosphere. This can be removed to make additions or to wash the cells with fresh medium, either of which can be accomplished using a standard pipettor.

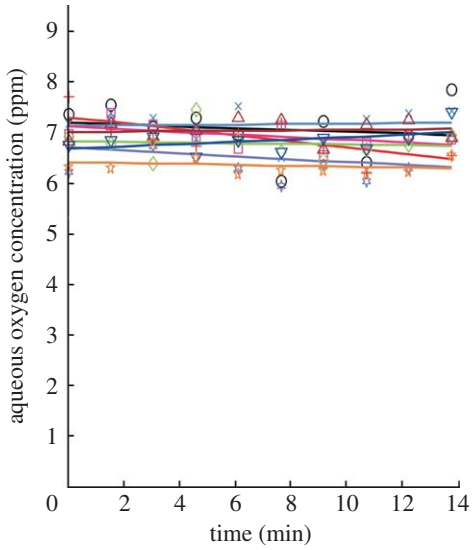

Figure 3. Measurement of oxygen concentration in wells that were first sealed under ambient oxygen conditions and then subjected to a low (0%)-oxygen environment, demonstrating sealing. Circle, well 1; plus, well 2; six-tailed star, well 3; cross, well 4; square, well 5; diamond, well 6; up triangle, well 7; down triangle, well 8; five-tailed star, well 9.

2.3. Actuator system

An actuator system (AS) was developed in order to diffusionally isolate the microwells within the LCA (figure 1). The AS consisted of a piston mounted to a manual actuator. For the piston, 0.6 cm stainless-steel rods were tapered to approximately 3 mm in diameter at one end. A thin piece of PDMS, also approximately 3 mm in diameter and 0.4 mm deep, was then attached to the piston using a cyanoacrylate adhesive. A 3 mm$\times$ 3 mm$\times$500 µm piece of borosilicate glass was then attached to the PDMS. The PDMS was used as a compliant layer to help ensure that the borosilicate glass and the microwell chip were coplanar during the sealing process. This system replaced the gold foil seal described previously (Molter *et al.* 2008). Before experimental use, the borosilicate glass lid of the piston assembly was rinsed with 70% EtOH in H_2O and then with deionized water to remove any particulates or dust that may have settled onto the lid. Cleaning the lid helped to ensure an adequate seal and that no contamination of the cells occurred.

The AS was developed in such a way that the tapered end of the piston would constantly remain coaxial to the microscope objective, ensuring that the field of view for the user was also the same area to be sealed. The vertical movement of the piston was controlled using a precision linear stage, a lead screw and a hand crank, keeping the necessary components coaxial. A load cell (Cooper Instruments and Systems, Warrenton, VA, USA; LPM 510 25 lb and DCM 490) was placed within the AS to allow for real-time measurements of the force being applied. The load cell was connected to an input–output box (I/O Tech, Cleveland, OH, USA; DaqTemp 14A), which was interfaced through a computer via I/O Tech DaqView software. The force that was applied was also recorded. As can be seen in figure 2, the AS was secured to the microscope platform, which allowed for up to 6.8 kg of force with this system to be used when diffusionally isolating the microwells.

2.4. Temperature control

All oxygen consumption experiments were performed at 37°C on a Zeiss 510 META Laser Scanning Microscope (LSM; Zeiss, Thornwood, NY, USA). The temperature was maintained by using an in-house developed heating unit. A polycarbonate box was made to surround the microscope on all sides, with carefully located access ports that could be opened and closed to allow full access to the microscope and all other components located within the enclosed system (figure 2). The heat was provided by three heater elements (Omega Engineering, Stamford, CT, USA; Omegalux CIR-1040/120V), with each individual element coupled to a standard computer fan. The fan–heater modules were strategically placed inside the enclosure to allow for optimal heating and heat distribution. The modules were attached to the enclosure by a PDMS union, which greatly reduced the vibrations from the fans and increased the clarity of the images acquired by the LSM.

The heaters were controlled by an Omega temperature controller (Omega Engineering; CN8241-DC1). The temperature controller is set to a target temperature of 37°C. A thermocouple connected to the controller closes a feedback loop using a standard proportional–integral–derivative (PID) controller (figure 2). The temperature stability of the environmental chamber was monitored using up to 12 thermocouples. After temperature equilibration was reached (approx. 30 min), the monitored temperature had a standard deviation of 0.11°C over a period of 12 hours.

2.5. Cell line and growth conditions

The macrophage-like cell line RAW 267.4 was acquired from the American Type Culture Collection. Cells were cultured at 37°C under 5% CO_2 in Dulbecco's minimal essential medium (DMEM: Gibco BRL, Carlsbad, CA, USA) supplemented with 10% FBS, 5 mM HEPES, 0.2 mg ml^{-1} L-glutamine, 0.05 mM β-mercaptoethanol, 50 mg ml^{-1} gentamicin sulphate and 10 000 U ml^{-1} penicillin and streptomycin (Fink & Cookson 2006).

2.6. Dyes and cell seeding

Cell deposition by random seeding was used to deposit approximately one cell per microwell. Borosilicate chips were placed into 24-well tissue culture grade polystyrene plates (353047, BD Biosciences, San Jose, CA, USA). Approximately 1×10^4 cells in a 1 ml aliquot of culture medium were seeded into the wells, and the plates were incubated overnight at 37°C. Calcein AM (λ_{ex}=494 nm, λ_{em}=517 nm, C1430, Invitrogen) and SYTOX orange (λ_{ex}=547 nm, λ_{em}=570 nm, S11368, Invitrogen) were selected as the live and dead cell stains, respectively. Calcein AM was excited with a 488 nm argon laser and detected in channel 2 of the LSM. SYTOX orange was excited via a 543 nm helium–neon laser and detected in channel 3 of the LSM.

2.7. Data acquisition

Detailed descriptions of the data acquisition and sensor calibration have been previously reported (Molter *et al.* 2008). The excitation and emission maxima for the Pt-porphyrin are approximately 390 and 650 nm, respectively. In order to determine the oxygen concentration within a microwell, a phase modulation technique was established (Molter *et al.* 2008). A gated 405 nm diode laser (PPMT LD1539, Power Technology, Inc., Alexander, AR, USA) coupled to the rear port of the microscope was used to excite the oxygen sensor. An ICCD camera (Andor iStar DH734-18F, Andor Technology, South Windsor, CT, USA) connected to the base port of the microscope was used to collect the emission signal. A 585 nm long-pass filter was used to remove any reflected excitation signal from the data collection. The appropriate timing for both the laser and camera was achieved by connecting each element by a coaxial connector to a pulse–delay generator (BNC 555, Berkeley Nucleonics Corporation, San Rafael, CA, USA). An arbitrary function generator (AFG310, Tektronix, Inc.,

Irvine, CA, USA) was used to trigger the delay generator, ensuring the correct timing for signal generation and data collection. Standard blood gas calibration cylinders of 0, 10 and 20% O_2, with 5% CO_2 and N_2 balance, were used to calibrate the oxygen sensor.

2.8. Oxygen consumption experiments

The heating unit, laser, LSM and ICCD camera were initiated and the desired piston was secured into the AS and allowed to equilibrate to 37°C. During the system equilibration, 4 ml of cell culture medium was injected into the macrowell chamber and was placed within the microscope enclosure. After equilibration was achieved, a previously seeded chip was placed into the LCA and Calcein AM and SYTOX orange were added. The LCA was covered and a humidified 20% O_2/5% CO_2/N_2-balance gas line was inserted into the LCA, gently bathing the media. The entire system was allowed to equilibrate for at least 30 min before any measurements were taken. The ICCD camera was set to a 10×10 pixel bin size for all oxygen consumption experiments.

After the equilibration, a 3×3 section of microwells was chosen for observation by manually centring the array within the field of view of a 10× objective using a mechanical x–y stage. The piston lid was lowered until a steady 6.8 kg force was reported by the load cell. The seal was optically verified (see below), the microwell array of interest was imaged with the LSM, the previously developed Andor basic software (Molter *et al.* 2008) was then initiated and the oxygen concentration monitoring began. After the oxygen consumption experiment was completed, a final LSM image was acquired to verify the location of cells within the microwells as well as to quantify the number of live cells that contributed to the oxygen consumption. After the LSM image was acquired, the piston assembly was raised until the microwells were completely unsealed yet with the borosilicate seal kept in solution to avoid drying and subsequent crystallization of medium on the sealing surface. Once the piston was raised, the next region of interest was selected and the oxygen consumption measurement process was repeated. The oxygen consumption measurements on both 3×3 microwell arrays were repeated four times.

2.9. Seal confirmation

In order for the oxygen consumption data to be verified, it was imperative to prove that the AS does indeed diffusionally isolate each microwell within the LCA. Microwell leak tests were carried out both visually and experimentally. During experimental seal verification, microwells submerged in water containing 20% ambient oxygen were sealed with the AS (figure 3). The water outside of the sealed wells was then equilibrated to 0% oxygen and the oxygen concentration inside the sealed wells was monitored over time to observe any change in the sealed microwells from the original 20% oxygen level. The oxygen concentration was monitored for the same duration as a full oxygen consumption experiment, approximately 15 min. During visual seal verification, the glass–glass interface between the microwell lips and the AS lid was imaged using an argon laser (488 nm) on the LSM (figure 4). Concentric line patterns were observed around the microwells when the system was sealed. The lines are created by constructive and destructive interference of laser light reflecting off the chip and lid surface boundaries, similar to what is observed for Newton's rings (Cloud 2003). A highly symmetrical pattern was observed when uniform sealing of the microwells was achieved, with poor sealing indicated by an asymmetrical pattern.

3. RESULTS AND DISCUSSION

3.1. System characterization

In order to improve system performance and validate the system and the oxygen sensor, a systematic analysis of several variables was performed on the Andor iStar ICCD, the excitation source and the microscope. The parameters analysed for the ICCD include the effects of the thermoelectric cooler, the pixel bin size, the system gain, inherent delays within the Andor system, the number of accumulations at each step within a kinetic series and the operating frequency of the system. The location of the microwells within the field of excitation and the focus plane of the microscope were also examined. The stability of the 405 nm diode laser used as the excitation source was also investigated. Finally, the long-term stability of the oxygen concentration determination was studied. Sixty successive measurements of the same sensors had an average coefficient of variance of 3.2%, and for similar measurements carried out on different days it was 3.3%. The results of all of these analyses allowed for dramatic improvement of the experimental parameters required for phosphorescence monitoring and led to the development of the final method, which is detailed in §2.

3.2. System calibration

As described in §2.7, standard blood gas calibration cylinders of 0, 10 and 20% O_2, with 5% CO_2 and N_2 balance, were used to calibrate the system. As reported previously, an excellent correlation was observed using a modified Stern–Volmer equation that accounts for multiple fluorescing regions within the oxygen-sensitive microspheres (Molter *et al.* 2008).

3.3. Seal confirmation

As described previously, microwells were visually confirmed to be sealed by observing whether concentric line patterns were created when the glass–glass interface between the microwell lips and the AS lid was imaged using an argon laser (488 nm) on the LSM (figure 4).

A dirty glass lid, uneven positioning of the PDMS conformal layer, residual gold from the photolithographic process on the well lips and excess cellular debris were observed to be the most common causes for inadequate sealing.

In addition to visual seal test confirmation, experimental seal testing was conducted by sealing water at 20% oxygen inside the microwells, equilibrating the

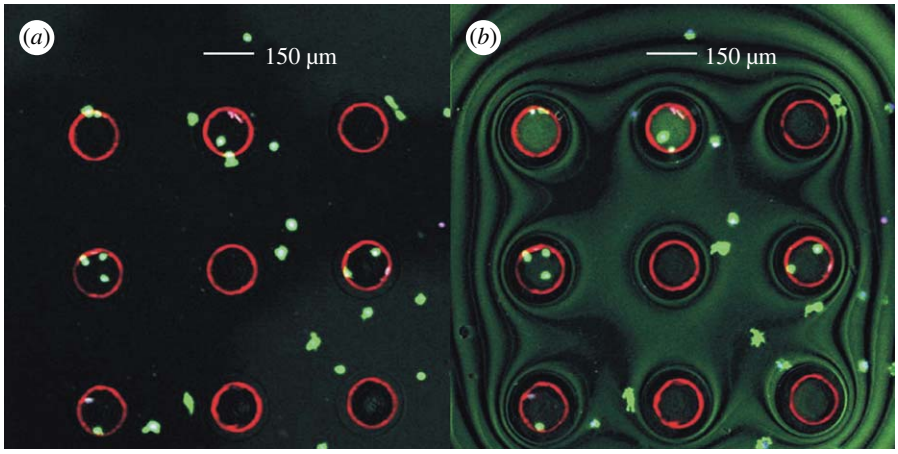

Figure 4. (*a*) An LSM image of unsealed microwells showing the presence of the deposited Pt-porphyrin microspheres and healthy mouse macrophage stained with Calcein AM live stain in green. (*b*) An LSM image of sealed microwells showing the deposited sensors and the seeded macrophages. The symmetric wavy lines are indicative of an adequately sealed system.

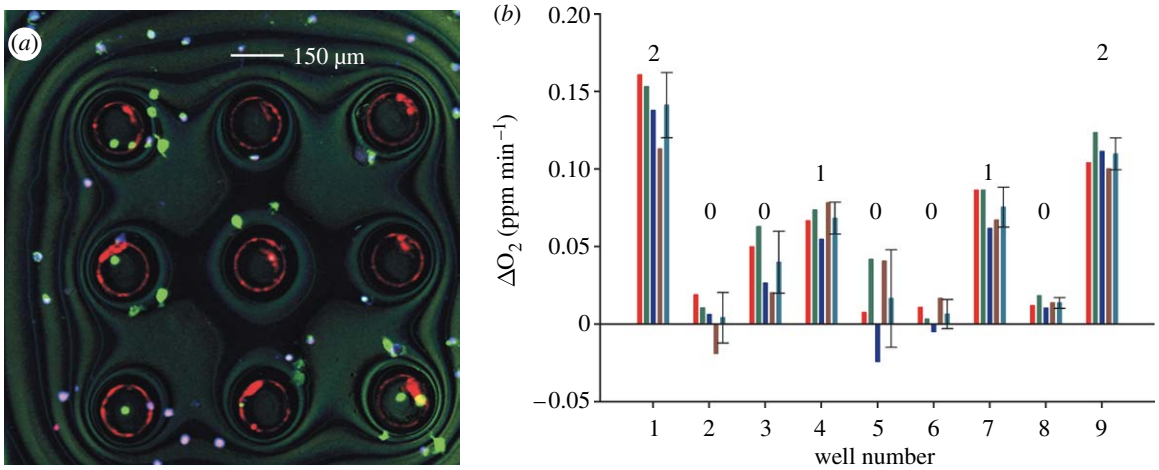

Figure 5. (*a*) An LSM image identifying the number of live cells present per microwell for an oxygen consumption experiment. Live cells are reported to be green, dead cells appear to be purple colour and the Pt-porphyrin rings are present in red. (*b*) The corresponding repetitive oxygen consumption slopes found from the isolated system are shown on the left.

surrounding water to 0% oxygen and observing any change in the oxygen inside the sealed microwells. As shown in figure 3, the oxygen concentration during these seal tests remained virtually constant over the 14 min duration of this experiment, with an average standard deviation of 0.40 ppm for each well measured. In cases in which the microwells were not sealed, the reported oxygen concentration quickly approached 0 ppm (data not shown).

3.4. Repeatability of oxygen consumption results

The system as described above was used to measure oxygen consumption of cells in the microwell arrays. Two array locations on one chip were measured, for a total of 18 wells, 9 with no cells, 6 with one cell and 3 with two cells. Repeatability was tested by carrying out oxygen consumption experiments with four sequential measurements of each cell. As shown in figure 5 and table 1, it was possible to measure oxygen consumption on wells with single cells. The replicate measurements showed good reproducibility, with standard deviations in most cases being within 30% of the average (table 1). In addition, no trends were consistently observed in the rates measured in the subsequent oxygen consumption measurements of the same cells, suggesting that the measurement itself does not significantly affect the oxygen consumption rate, either positively (stimulatory) or negatively (inhibitory).

3.5. Oxygen consumption rate measurement correlations with cell number

The 72 measurements shown in table 1 were plotted against the number of cells. An excellent correlation between the determined slope and the corresponding number of cells within the respective microwell (0, 1 or 2) was observed (figure 6). These results further validate the system for single-cell oxygen consumption measurements. A comparison of the results from the two array locations shows that they were similar to each other, within the standard deviation of the measurements (tables 1 and 2). This result is significant and suggests that this system can be used to compare single-cell respiration rates of a large number of single cells in multiple arrays. Although other methods are not available to test these results at the single-cell level,

Table 1. Repetitive oxygen consumption experiments for arrays 1 and 2.

array	microwell	no. of cells	rate 1[a]	rate 2[a]	rate 3[a]	rate 4[a]	average[a]	s.d.
1	1	2	0.161	0.153	0.138	0.113	0.141	0.021
	2	0	0.019	0.010	0.006	−0.019	0.004	0.016
	3	0	0.050	0.063	0.026	0.020	0.040	0.020
	4	1	0.067	0.074	0.055	0.078	0.068	0.010
	5	0	0.007	0.042	−0.024	0.041	0.016	0.031
	6	0	0.011	0.003	−0.005	0.017	0.006	0.009
	7	1	0.086	0.086	0.062	0.067	0.075	0.013
	8	0	0.012	0.018	0.010	0.014	0.014	0.003
	9	2	0.104	0.123	0.111	0.100	0.110	0.010
2	1	1	0.071	0.070	0.057	0.059	0.064	0.007
	2	0	−0.003	0.019	0.055	0.002	0.018	0.026
	3	2	0.212	0.177	0.129	0.150	0.167	0.036
	4	1	0.090	0.072	0.094	0.046	0.075	0.022
	5	0	0.018	0.014	0.024	0.014	0.018	0.005
	6	0	0.003	0.006	−0.017	0.049	0.010	0.028
	7	1	0.052	0.018	0.055	0.082	0.052	0.026
	8	0	0.030	0.025	0.031	−0.017	0.017	0.023
	9	1	0.125	0.063	0.058	0.065	0.078	0.031

[a] ppm min^{-1}.

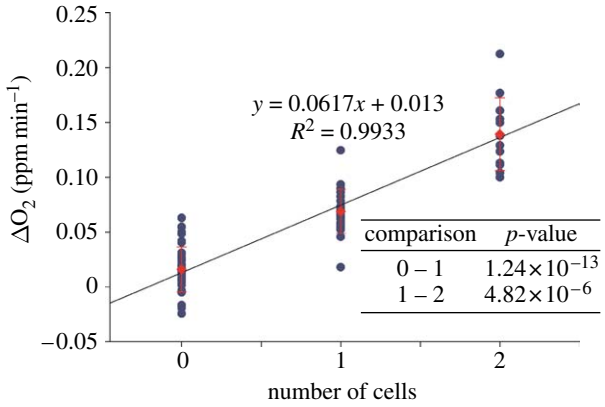

Figure 6. The reported oxygen consumption rates plotted against the number of cells present. Circle, consumption rate; diamond, average.

bulk oxygen consumption rate measurements have been previously validated with a Clark electrode (Strovas *et al.* 2006).

As can be seen from figure 6, a small rate of oxygen consumption is observed in the absence of cells. This is not due to leaks, but is an inherent property of the sensor beads and has been referred to as the induction effect (Hicks *et al.* 1988; Sinaasappel & Ince 1996; Liu & Sullivan 2004). This induction effect can limit the usefulness of the approach, if high light intensities are used (Mitra & Foster 2000). In this test light intensities were kept to a minimum. Although the average induction rate is lower than the average of single cells, significant overlap occurs with about half of the measurements. Therefore, comparing rates of individual cells with each other requires high numbers of measurements. Further modifications, such as decreasing the volume of the well or using different formulations of the porphyrin sensor, to increase the difference between the zero-cell and single-cell measurements will increase the applicability and usability of this system for heterogeneity assessments of single-cell and bulk-cell populations.

Table 2. Oxygen consumption rate comparison.

no. of cells	0	1	2	2/2[a]
average[b]	0.016	0.069	0.139	0.070
s.d.	0.020	0.020	0.033	0.017

[a] Divided by 2 to normalize to one cell.
[b] ppm min^{-1}.

4. CONCLUSIONS

The development and application of a system capable of monitoring the respiration rates from multiple diffusionally isolated single cells were shown. Sealing of the microwells can be quickly determined, thus little experimental time is lost due to improper seals. Using the automation of the LSM, multiple arrays of cells could be investigated in a short period of time, increasing the overall throughput of the system. The system was made even more robust by the in-house development of the LCA and AS, both of which easily allow for the insertion of new seals and new sets of seeded microwell arrays. The oxygen-sensitive characteristics of Pt-porphyrin-embedded 1 μm polystyrene microspheres were used to monitor the local oxygen concentration over time using a previously developed phase modulation technique (Molter *et al.* 2008). Using this technique and the CIS, multiple oxygen consumption experiments were carried out on the same set of cells with a high level of reproducibility.

The development of this single-cell observation system has allowed for non-invasive reproducible measurements of oxygen consumption rates in individual cells in real time. The ability to reproducibly measure physiological parameters such as oxygen consumption rates in single cells opens up a new line of enquiry into the relationship of pre-existing physiological state with cellular response. At the Microscale Life Sciences Center (MLSC), we are currently studying heterogeneity in inflammatory cell

death pathways (Fink & Cookson 2005) and in cancer progression, in Barrett's oesophagus (Maley *et al.* 2006). By assessing physiological state and correlating that with the type of response obtained to a stimulus, either a death stimulus or a known risk factor, it may be possible to identify new targets for diagnostics and therapeutic agents, as well as new insights into disease pathways that are currently obscured by data obtained with bulk cultures.

The authors would like to thank Dr Shih-hui Chao for his helpful discussions. This work was supported by a grant from the Centers of Excellence in Genomic Science (CEGS), the MLSC, NIH National Human Genome Research Institute (NHGRI; P50 HG 002360).

REFERENCES

Amao, Y., Asai, K. & Okura, I. 2000 Oxygen sensing based on lifetime of photoexcited triplet state of platinum porphyrin–polystyrene film using time-resolved spectroscopy. *J. Porphyr. Phthalocya.* **4**, 292–299. (doi:10.1002/(SICI)1099-1409(200004/05)4:3<292::AID-JPP216>3.0.CO;2-W)

Armaroli, N. 2003 From metal complexes to fullerene arrays: exploring the exciting world of supramolecular photochemistry fifteen years after its birth. *Photochem. Photobiol. Sci.* **2**, 3–87. (doi:10.1039/b210569a)

Balaban, N. Q., Merrin, J., Chait, R., Kowalik, L. & Leibler, S. 2004 Bacterial persistence as a phenotypic switch. *Science* **305**, 1622–1625. (doi:10.1126/science.1099390)

Bugger, H., Chemnitius, J.-M. & Doenst, T. 2006 Differential changes in respiratory capacity and ischemia tolerance of isolated mitochondria from atrophied and hypertrophied hearts. *Metabolism* **55**, 1097–1106. (doi:10.1016/j.metabol.2006.04.005)

Carano, M., Holt, K. B. & Bard, A. J. 2003 Scanning electrochemical microscopy. 49. Gas-phase scanning electrochemical microscopy measurements with a Clark oxygen ultramicroelectrode. *Anal. Chem.* **75**, 5071–5079. (doi:10.1021/ac034546q)

Cloud, G. 2003 Optical methods in experimental mechanics—part 5—a classic interferometry: Newton's rings. *Exp. Tech.* **27**, 17–19. (doi:10.1111/j.1747-1567.2003.tb00094.x)

Dy, E. S. & Kasai, H. 2005 Characterization of platinum porphyrins and its interaction with oxygen by density functional theory. *e-J. Surf. Sci. Nanotechnol.* **3**, 473–475. (doi:10.1380/ejssnt.2005.473)

Fink, S. L. & Cookson, B. T. 2005 Apoptosis, pyroptosis, and necrosis: mechanistic description of dead and dying eukaryotic cells. *Infect. Immun.* **73**, 1907–1916. (doi:10.1128/IAI.73.4.1907-1916.2005)

Fink, S. L. & Cookson, B. T. 2006 Caspase-1-dependent pore formation during pyroptosis leads to osmotic lysis of infected host macrophages. *Cell. Microbiol.* **8**, 1812–1825. (doi:10.1111/j.1462-5822.2006.00751.x)

Gao, N., Zhao, M., Zhang, X. & Jin, W. 2006 Measurement of enzyme activity in single cells by voltammetry using a microcell with a positionable dual electrode. *Anal. Chem.* **78**, 231–238. (doi:10.1021/ac051178c)

Hartmann, P. & Trettnak, W. 1996 Effects of polymer matrixes on calibration functions of luminescent oxygen sensors based on porphyrin ketone complexes. *Anal. Chem.* **68**, 2615–2620. (doi:10.1021/ac960008k)

Hicks, J. M., Urbach, L. E., Plummer, E. W. & Dai, H. L. 1988 Can pulsed laser excitation of surfaces be described by a thermal-model. *Phys. Rev. Lett.* **61**, 2588–2591. (doi:10.1103/PhysRevLett.61.2588)

Kelly, C. D. & Rahn, O. 1932 The growth rate of individual bacterial cells. *J. Bacteriol.* **23**, 147–153.

Kamme, F. *et al.* 2003 Single-cell microarray analysis in hippocampus CA1: demonstration and validation of cellular heterogeneity. *J. Neurosci.* **23**, 3607–3615.

Lahdesmaki, I., Scampavia, L. D., Beeson, C. & Ruzicka, J. 1999 Detection of oxygen consumption of cultured adherent cells by bead injection spectroscopy. *Anal. Chem.* **71**, 5248–5252. (doi:10.1021/ac990712b)

Land, S. C., Porterfield, D. M., Sanger, R. H. & Smith, P. J. 1999 The self-referencing oxygen-selective microelectrode: detection of transmembrane oxygen flux from single cells. *J. Exp. Biol.* **202**(Pt 2), 211–218.

Lidstrom, M. E. & Meldrum, D. R. 2003 Life-on-a-chip. *Nat. Rev. Microbiol.* **1**, 158–164. (doi:10.1038/nrmicro755)

Liu, T. & Sullivan, J. P. 2004 *Pressure and temperature sensitive paints*. Berlin, Germany: Springer.

Lu, H. & Gratzl, M. 1999 Monitoring drug efflux from sensitive and multidrug-resistant single cancer cells with microvoltammetry. *Anal. Chem.* **71**, 2821–2830. (doi:10.1021/ac9811773)

Maley, C. C. *et al.* 2006 Genetic clonal diversity predicts progression to esophageal adenocarcinoma. *Nat. Genet.* **38**, 468–473. (doi:10.1038/ng1768)

Mitra, S. & Foster, T. H. 2000 Photochemical oxygen consumption by a porphyrin phosphorescent probe in two model systems. *Biophys. J.* **78**, 2597–2605.

Molter, T. W. 2006 *Automation of single cell oxygen consumption experiments*, p. 114. Seattle, WA: University of Washington.

Molter, T. W., Holl, M. R., Dragavon, J. M., McQuaide, S. C., Anderson, J. B., Young, A. C., Burgess, L. W., Lidstrom, M. E. & Meldrum, D. R. 2008 A new approach for measuring single cell oxygen consumption rates. *IEEE Trans. Autom. Sci. Eng.* **5**, 32–42. (doi:10.1109/TASE.2007.909441)

Porterfield, D. M. & Smith, P. J. S. 2000 Single-cell, real-time measurements of extracellular oxygen and proton fluxes from *Spirogyra grevilleana*. *Protoplasma* **212**, 80–88. (doi:10.1007/BF01279349)

Ramamoorthi, R. & Lidstrom, M. E. 1995 Transcriptional analysis of *pqqD* and study of the regulation of pyrroloquinoline quinone biosynthesis in *Methylobacterium extorquens* AM1. *J. Bacteriol.* **177**, 206–211.

Reece, J. S., Miller, M. J., Arnold, M. A., Waterhouse, C., Delaplaine, T., Cohn, L. & Cannon, T. 2003 Continuous oxygen monitoring of mammalian cell growth on space shuttle mission STS-93 with a novel radioluminescent oxygen sensor. *Appl. Biochem. Biotechnol.* **104**, 1–11. (doi:10.1385/ABAB:104:1:1)

Shonat, R. D. & Kight, A. C. 2003 Oxygen tension imaging in the mouse retina. *Ann. Biomed. Eng.* **31**, 1084–1096. (doi:10.1114/1.1603256)

Sinaasappel, M. & Ince, C. 1996 Calibration of Pd-porphyrin phosphorescence for oxygen concentration measurements *in vivo*. *J. Appl. Physiol.* **81**, 2297–2303.

Strovas, T. J., Dragavon, J. M., Hankins, T. J., Callis, J. B., Burgess, L. W. & Lidstrom, M. E. 2006 Measurement of respiration rates of *Methylobacterium extorquens* AM1 cultures by use of a phosphorescence-based sensor. *Appl. Environ. Microbiol.* **72**, 1692–1695. (doi:10.1128/AEM.72.2.1692-1695.2006)

Strovas, T. J., Sauter, L. M., Guo, X. F. & Lidstrom, M. E. 2007 Cell-to-cell heterogeneity in growth rate and gene expression in *Methylobacterium extorquens* AM1. *J. Bacteriol.* **189**, 7127–7133. (doi:10.1128/JB.00746-07)

Verstovsek, S., Zaleskis, G., Maccubbin, D. L., Mihich, E. & Ehrke, M. J. 1994 Lipopolysaccharide and splenic tumoricidal macrophage activation. *J. Leukoc. Biol.* **56**, 714–722.

Vinogradov, S. A., Fernandez-Searra, M. A., Dugan, B. W. & Wilson, D. F. 2001 Frequency domain instrument for measuring phosphorescence lifetime distributions in heterogeneous samples. *Rev. Sci. Instrum.* **72**, 3396–3406. (doi:10.1063/1.1386634)

von Heimburg, D., Hemmrich, K., Zachariah, S., Staiger, H. & Pallua, N. 2005 Oxygen consumption in undifferentiated versus differentiated adipogenic mesenchymal precursor cells. *Respir. Physiol. Neurobiol.* **146**, 107–116. (doi:10.1016/j.resp.2004.12.013)

Yasukawa, T., Kaya, T. & Matsue, T. 2000 Characterization and imaging of single cells with scanning electrochemical microscopy. *Electroanalysis* **12**, 653–659. (doi:10.1002/1521-4109(200005)12:9<653::AID-ELAN653>3.0.CO;2-S)